Engineering Letters

Stability and Bifurcation in Lotka-Volterra Amensalism Model with Saturated Wind Effect

Fengde Chen, Yuting Huang and Guangwen He

***Abstract*—Wind facilitates pathogen/pest dispersal and ecosystem destabilization, yet existing models frequently neglect saturation effects under extreme wind speeds. This paper studies an amensalism population model with a saturated wind effect, aiming to explore the nonlinear impact of wind on interspecific interactions in ecosystems. Wind plays a crucial role in ecosystems, not only affecting the diffusion and distribution of populations but also potentially altering population dynamics by enhancing or weakening interspecific interactions. However, existing research often overlooks the saturation effect of wind on interspecific interactions, where the impact of wind on interspecific interactions tends to stabilize when wind speed is too high. Based on the classical Lotka-Volterra amensalism model, this paper introduces a wind modulation function with a saturation effect to describe the nonlinear impact of wind speed on the amensalism coefficient. Through theoretical analysis and extensive numerical simulations, we investigate the dynamic behavior of the model and explore the impact of wind speed on the long-term stability of the victim and amensalist populations. The results show that the saturation effect of wind on amensalism significantly alters the population's equilibrium state and stability conditions. Numerical simulations validate the theoretical findings and reveal the sensitivity of population dynamics to key parameters, including wind speed w, saturation coefficient κ, and wind-enhanced coefficient δ. Specifically, we demonstrate how varying these parameters influences the coexistence or extinction of the victim population, with critical thresholds identified for ecological sustainability. The model proposed in this paper provides a new theoretical framework for understanding the role of wind in ecosystems and offers scientific support for formulating relevant ecological management strategies.**

***Index Terms*—Lotka-Volterra amensalism model, local stability, global stability, saturated wind effect, bifurcation**

I. INTRODUCTION

A. Research Background and Significance

POPULATION dynamics in ecosystems are influenced by various biological and abiotic factors, among which interspecific interactions (such as competition, predation, and amensalism) are one of the core mechanisms determining population dynamics. Amensalism is a special type of interspecific interaction where one population (the amensalist population) negatively affects another (the victim population) without being affected by the victim population. This relationship is widespread, such as the feeding behavior of certain insects on plants or the infection process of pathogens on hosts. Over the past decade, many scholars have conducted in-depth research on the dynamic behaviors of amensalism population models[1]-[45], yielding numerous valuable findings. However, to date, no scholar has explored the impact of wind on the dynamic behaviors of amensalism ecosystems.

Wind significantly influences ecosystems. It affects the diffusion and distribution of populations (e.g., seed dispersal, insect migration) and may also indirectly influence population dynamics by altering the intensity of interspecific interactions. For example, wind can help pathogens or insects spread to new areas, enhancing their negative impact on the victim population. Although wind, as an abiotic factor, significantly impacts ecosystems, related theoretical research has been scarce. It was only recently that biomathematicians began to build upon classical predator-prey models by incorporating the influence of wind, proposing various predator-prey population models to explore their dynamic behaviors [46]-[52]. However, most existing research ignores the nonlinear impact of wind on interspecific interactions, especially the saturation effect that may occur when wind speed is too high. This saturation effect is significant in ecosystems because excessively high wind speeds may cause the enhancing effect of amensalism to stabilize or weaken due to physical damage.

B. Significance of the Problem

The traditional Lotka-Volterra amensalism model, while capable of describing interspecific interactions, fails to consider the modulation effect of wind on these interactions. Moreover, the effect of wind in existing models is often simplified as a linear relationship, which does not align with the nonlinear phenomena observed in real ecosystems. This is crucial for predicting population dynamics under varying wind conditions, which is essential for ecosystem management.

This study aims to fill this gap by introducing a wind modulation function with a saturation effect, thereby establishing a more realistic amensalism population model. This model can not only describe the enhancing effect of wind speed on amensalism but also reflect the saturation phenomenon when wind speed is too high. Through this model, we can more accurately predict the impact of wind on population dynamics and provide theoretical support for the management and conservation of ecosystems.

C. Model Innovations

The main innovations of this paper include:

- **Introduction of Saturation Effect**: By introducing a wind modulation function with a saturation effect, the nonlinear impact of wind speed on amensalism is characterized.

Manuscript received March 3, 2025, revised May 2, 2025. This work is supported by the Natural Science Foundation of Fujian Province(2024J01273).

F. D. Chen is a professor of College of Mathematics and Statistics, Fuzhou University, Fuzhou, CHINA (e-mail: fdchen@fzu.edu.cn).

Y. T. Huang is a postgraduate student of College of Mathematics and Statistics, Fuzhou University, Fuzhou, CHINA (e-mail: 1104943637@qq.com).

G. W. He is a postgraduate student of College of Mathematics and Statistics, Fuzhou University, Fuzhou, CHINA (e-mail: 594047408@qq.com).

- **Theoretical Analysis**: A detailed theoretical analysis of the model's equilibrium points and stability is conducted, revealing the mechanism of wind speed's impact on population dynamics.
- **Numerical Simulation**: Numerical simulations are used to validate the theoretical results and explore the dynamic behavior of populations under different wind speeds.

D. Research Objectives

The research objectives of this paper include:

- Establishing an amensalism population model with a saturated wind effect to describe the nonlinear impact of wind speed on interspecific interactions.
- Analyzing the equilibrium points and stability of the model to explore the mechanism of wind speed's impact on population dynamics.
- Validating the theoretical results through numerical simulations and discussing the ecological significance of the model.
- Providing scientific support for the formulation of relevant ecological management strategies.

E. Paper Structure

The structure of this paper is as follows: Chapter 1 is the introduction, which presents the research background, significance of the problem, and model innovations; Chapter 2 describes the model construction process in detail; Chapter 3 provides a theoretical analysis of the model's equilibrium points and stability; Chapter 4 validates the theoretical results through numerical simulations; Chapter 5 summarizes the research conclusions and discusses the ecological significance and application prospects of the model.

II. MODEL CONSTRUCTION

This paper is based on the classical Lotka-Volterra commensalism model, incorporating a wind modulation function with a saturation effect to describe the nonlinear impact of wind speed on the commensalism coefficient. The model construction process is as follows:

1) **Dynamic of the victim population** N_1:
    a) The victim population N_1 grows under resource limitations and negative effects from N_2;
    b) Wind further suppresses the growth of N_1 by enhancing the commensal effect $\alpha(w)$.
2) **Dynamic of the commensal population** N_2:
    a) The growth of the commensal population N_2 is solely constrained by resource limitations and is unaffected by the victim population N_1.
    b) The direct impact of wind on N_2 is neglected, and wind only indirectly affects N_1 through the commensal interaction.
3) **Effect of wind**:
    a) Wind enhances the negative impact of the commensal population N_2 on the victim population N_1;
    b) When the wind speed is too high, the commensal effect tends to saturate, avoiding the unreasonable phenomenon of infinite enhancement.

Based on the above ecological background and model construction, the proposed model is as follows:

$$\begin{aligned} \frac{dN_1}{dt} &= r_1N_1\left(1-\tfrac{N_1}{K_1}\right)-\alpha(w)N_1N_2, \\ \frac{dN_2}{dt} &= r_2N_2\left(1-\tfrac{N_2}{K_2}\right), \end{aligned} \tag{1}$$

where

$$\alpha(w)=\alpha_0\left(1+\frac{\delta w}{1+\kappa w}\right).$$

Here, r_1 represents the intrinsic growth rate of the victim population, with ecological significance being the maximum growth rate of N_1 under unlimited resources and the absence of the commensal population. K_1 denotes the environmental carrying capacity of the victim population, representing the maximum population size of N_1 under resource limitations in the absence of the commensal population. r_2 is the intrinsic growth rate of the commensal population, indicating the maximum growth rate of N_2 under unlimited resources. K_2 is the environmental carrying capacity of the commensal population, representing the maximum population size of N_2 in the absence of the victim population. α_0 is the baseline commensal effect coefficient without wind, quantifying the negative impact intensity of N_2 on N_1. δ is the wind-enhanced coefficient for the commensal effect, reflecting the degree to which wind speed w amplifies $\alpha(w)$. κ is the saturation coefficient, controlling the rate at which wind speed drives the commensal effect toward saturation—a larger κ implies a more pronounced saturation effect. Wind speed w ecologically represents the intensity of wind's influence on the commensal effect, which strengthens with higher wind speed but exhibits saturation.

III. EXISTENCE ANALYSIS OF EQUILIBRIUM POINTS

For system (1), let the equilibrium point be (N_1^*, N_2^*). It must satisfy:

$$\begin{aligned} &r_1N_1^*\left(1-\tfrac{N_1^*}{K_1}\right)-\alpha(w)N_1^*N_2^*=0, \\ &r_2N_2^*\left(1-\tfrac{N_2^*}{K_2}\right)=0. \end{aligned} \tag{2}$$

From the second equation of system (2), we obtain:

$$N_2^*=0$$

or

$$N_2^*=K_2.$$

Case 1: $N_2^*=0$ (Extinction of the amensalist population).

When $N_2^*=0$, the first equation of (2) simplifies to:

$$r_1N_1^*\left(1-\frac{N_1^*}{K_1}\right)=0.$$

Solutions are:

- $N_1^*=0$ (extinction of the victim population),
- $N_1^*=K_1$ (victim population reaches carrying capacity).

Thus, when $N_2^*=0$, the system has two equilibrium points:

$$(N_1^*, N_2^*)=(0,0) \quad \text{and} \quad (K_1,0).$$

Case 2: $N_2^*=K_2$ (Amensalist population reaches carrying capacity).

When $N_2^* = K_2$, the dynamic equation for N_1 becomes:

$$r_1 N_1^* \left(1 - \frac{N_1^*}{K_1}\right) - \alpha(w) N_1^* K_2 = 0.$$

If $N_1^* = 0$, the system has the boundary equilibrium point $(0, K_2)$. Assuming $N_1^* \neq 0$, divide both sides by N_1^*:

$$r_1 \left(1 - \frac{N_1^*}{K_1}\right) - \alpha(w) K_2 = 0.$$

Solving for N_1^*:

$$1 - \frac{N_1^*}{K_1} = \frac{\alpha(w) K_2}{r_1} \quad \Rightarrow \quad N_1^* = K_1 \left(1 - \frac{\alpha(w) K_2}{r_1}\right).$$

To ensure $N_1^* > 0$, the following condition must hold:

$$1 - \frac{\alpha(w) K_2}{r_1} > 0 \quad \Rightarrow \quad \alpha(w) K_2 < r_1.$$

Therefore, when $N_2^* = K_2$, the positive equilibrium point is:

$$(N_1^*, N_2^*) = \left(K_1 \left(1 - \frac{\alpha(w) K_2}{r_1}\right), K_2\right).$$

Summarizing the above analysis, we conclude:

Theorem 3.1. *System (1) always has the equilibrium points $E_0(0,0)$, $E_1(K_1,0)$, and $E_2(0,K_2)$. Additionally, if*

$$\alpha(w) K_2 < r_1 \tag{3}$$

holds, the system has a positive equilibrium point $E^*(N_1^*, N_2^*) = \left(K_1 \left(1 - \frac{\alpha(w) K_2}{r_1}\right), K_2\right)$.

IV. LOCAL STABILITY ANALYSIS OF EQUILIBRIUM POINTS

For the local stability of the system's equilibrium points, We find that the equilibrium points exhibit different stability properties depending on wind speed. Indeed, we have the following results:

Theorem 4.1. *$E_0(0,0)$ is an unstable source; $E_1(K_1,0)$ is a saddle point; if $\alpha(w)K_2 < r_1$, $E_2(0,K_2)$ is a saddle point (unstable). If $\alpha(w)K_2 > r_1$, then $\lambda_1 < 0$, and $E_2(0,K_2)$ becomes a stable node. The positive equilibrium $E^*(N_1^*, N_2^*)$, if it exists, is always a stable node.*

Proof. The Jacobian matrix J is given by:

$$J = \begin{pmatrix} \frac{\partial f}{\partial N_1} & \frac{\partial f}{\partial N_2} \\ \frac{\partial g}{\partial N_1} & \frac{\partial g}{\partial N_2} \end{pmatrix}$$

where

$$\begin{aligned} f(N_1, N_2) &= r_1 N_1 \left(1 - \tfrac{N_1}{K_1}\right) - \alpha(w) N_1 N_2, \\ g(N_1, N_2) &= r_2 N_2 \left(1 - \tfrac{N_2}{K_2}\right). \end{aligned} \tag{4}$$

Partial derivatives are calculated as:

$$\begin{aligned} \frac{\partial f}{\partial N_1} &= r_1 \left(1 - \tfrac{2N_1}{K_1}\right) - \alpha(w) N_2, \\ \frac{\partial f}{\partial N_2} &= -\alpha(w) N_1, \\ \frac{\partial g}{\partial N_1} &= 0, \\ \frac{\partial g}{\partial N_2} &= r_2 \left(1 - \tfrac{2N_2}{K_2}\right) \end{aligned} \tag{5}$$

At equilibrium $E_0(0,0)$, the Jacobian matrix is:

$$J(E_0(0,0)) = \begin{pmatrix} r_1 & 0 \\ 0 & r_2 \end{pmatrix}$$

with eigenvalues:

$$\lambda_1 = r_1, \quad \lambda_2 = r_2.$$

Since $\lambda_1, \lambda_2 > 0$, $E_0(0,0)$ is an unstable source.

At equilibrium $E_1(K_1, 0)$, the Jacobian matrix is:

$$J(K_1, 0) = \begin{pmatrix} -r_1 & -\alpha(w) K_1 \\ 0 & r_2 \end{pmatrix}$$

with eigenvalues:

$$\lambda_1 = -r_1, \quad \lambda_2 = r_2.$$

Since $\lambda_1 < 0$ and $\lambda_2 > 0$, $E_1(K_1, 0)$ is a saddle point, which is unstable.

At equilibrium $E_2(0, K_2)$, the Jacobian matrix is:

$$J(E_2(0, K_2)) = \begin{pmatrix} r_1 - \alpha(w) K_2 & 0 \\ 0 & -r_2 \end{pmatrix}$$

with eigenvalues:

$$\lambda_1 = r_1 - \alpha(w) K_2, \quad \lambda_2 = -r_2.$$

Since $\lambda_2 = -r_2 < 0$, the stability depends on λ_1:

- If $\alpha(w)K_2 < r_1$, $\lambda_1 > 0$, making $E_2(0, K_2)$ a saddle point.
- If $\alpha(w)K_2 > r_1$, $\lambda_1 < 0$, making $E_2(0, K_2)$ a stable node.

For the positive equilibrium $E^*(N_1^*, N_2^*)$, the Jacobian matrix is:

$$J(E^*(N_1^*, K_2)) = \begin{pmatrix} r_1 \left(1 - \frac{2N_1^*}{K_1}\right) - \alpha(w) K_2 & -\alpha(w) N_1^* \\ 0 & -r_2 \end{pmatrix}$$

Substituting $N_1^* = K_1 \left(1 - \frac{\alpha(w) K_2}{r_1}\right)$, the eigenvalues are:

$$\lambda_1 = -r_1 + \alpha(w) K_2, \quad \lambda_2 = -r_2.$$

Since $\alpha(w)K_2 < r_1$ (existence condition), $\lambda_1 < 0$. Thus, E^* is a stable node.
Theorem 4.1 is proved.

Remark 4.1. Ecological implications:

- **Coexistence stability**:
  - At low wind speeds ($\alpha(w)K_2 < r_1$), the victim population stably coexists with the amensalist population.
  - At critical wind speed $\alpha(w)K_2 = r_1$, a transcritical bifurcation occurs, leading to victim population extinction.
- **Management implications**:
  - Controlling wind speed or reducing $\alpha(w)$ (e.g., isolating pathogens) ensures $\alpha(w)K_2 < r_1$, maintaining ecological balance.
  - If $\alpha(w)K_2 \geq r_1$, interventions are needed to prevent victim extinction.

V. GLOBAL STABILITY ANALYSIS

The previous section discussed the local stability of equilibrium points. Here, we further establish sufficient conditions for the global stability of these points.

A. Global Stability of the Boundary Equilibrium $E_2(0, K_2)$

Theorem 5.1. *When $\alpha(w)K_2 > r_1$, the boundary equilibrium $E_2(0, K_2)$ is globally asymptotically stable.*
Proof. For sufficiently small $\varepsilon > 0$, the condition $\alpha(w)K_2 > r_1$ implies:

$$\alpha(w)(K_2 - \varepsilon) > r_1 \tag{6}$$

Since the second equation of system (1) is independent and follows the classical logistic equation, for any $N_2(0) > 0$,

$$\lim_{t\to\infty} N_2(t) = K_2. \tag{7}$$

Thus, there exists $T_1 > 0$ such that for $t > T_1$,

$$N_2(t) > K_2 - \varepsilon. \tag{8}$$

Substituting (8) into the first equation of (1), for $t > T_1$,

$$\begin{aligned} \tfrac{dN_1}{dt} &= N_1\left[r_1\left(1 - \tfrac{N_1}{K_1}\right) - \alpha(w)N_2\right] \\ &\leq N_1\left[r_1\left(1 - \tfrac{N_1}{K_1}\right) - \alpha(w)(K_2 - \varepsilon)\right] \\ &\leq (r_1 - \alpha(w)(K_2 - \varepsilon))N_1. \end{aligned} \tag{9}$$

Combining with (6), as $t \to +\infty$,

$$N_1(t) \leq N_1(T_1)\exp\{(r_1 - \alpha(w)(K_2 - \varepsilon))(t - T_1)\} \to 0. \tag{10}$$

Theorem 5.1 is proved.

B. Global Stability of the Positive Equilibrium $E^*(N_1^*, K_2)$

Theorem 5.2 *When $\alpha(w)K_2 < r_1$, the positive equilibrium $E^*(N_1^*, K_2)$ is globally asymptotically stable.*
Proof. We first prove that solutions with initial conditions $N_1(0) > 0, N_2(0) > 0$ remain positive. Integrating both sides of system (1) from 0 to t leads to

$$\begin{aligned} N_1(t) &= N_1(0)\exp\left\{\textstyle\int_0^t F_1 dt\right\} > 0, \\ N_2(t) &= N_2(0)\exp\left\{\textstyle\int_0^t \left[r_2\left(1 - \tfrac{N_2}{K_2}\right)\right]dt\right\} > 0. \end{aligned} \tag{11}$$

where

$$F_1 = r_1\left(1 - \frac{N_1}{K_1}\right) - \alpha(w)N_2.$$

Next, we analyze the boundedness of solutions. From (7), for sufficiently small $\varepsilon > 0$, there exists $T_1 > 0$ such that for $t > T_1$,

$$N_2(t) < K_2 + \varepsilon, \tag{12}$$

From the second equation of (1),

$$\frac{dN_1}{dt} \leq r_1 N_1\left(1 - \frac{N_1}{K_1}\right), \tag{13}$$

implying

$$\limsup_{t\to+\infty} N_1(t) \leq K_1. \tag{14}$$

Thus, there exists $T_2 > T_1$ such that for $t > T_2$,

$$N_1(t) < K_1 + \varepsilon. \tag{15}$$

All solutions eventually enter the compact set $\Omega = [0, K_1 + \varepsilon] \times [0, K_2 + \varepsilon]$.

Consider the function $B(N_1, N_2) = \frac{1}{N_1 N_2}$. The divergence is:

$$\text{div}(B\mathbf{F}) = \frac{\partial}{\partial N_1}\left(B \cdot \frac{dN_1}{dt}\right) + \frac{\partial}{\partial N_2}\left(B \cdot \frac{dN_2}{dt}\right)$$

Substituting the equations:

$$\frac{\partial}{\partial N_1}\left(\frac{r_1(1 - N_1/K_1) - \alpha(w)N_2}{N_2}\right) = -\frac{r_1}{K_1 N_2},$$

$$\frac{\partial}{\partial N_2}\left(\frac{r_2(1 - N_2/K_2)}{N_1}\right) = -\frac{r_2}{K_2 N_1}.$$

In the first quadrant, the total divergence is:

$$\text{div}(B\mathbf{F}) = -\frac{r_1}{K_1 N_2} - \frac{r_2}{K_2 N_1} < 0.$$

By Dulac's criterion, there are no periodic orbits in Ω. Since the system is a 2D autonomous system with:

- Solutions confined to Ω,
- No periodic orbits,
- Unstable boundary equilibria E_0, E_1, E_2 (Theorem 4.1),

Corresponding to Dulac criterion[53], all trajectories must converge to the unique positive equilibrium E^*. Therefore, when $\alpha(w)K_2 < r_1$, E^* is globally asymptotically stable in the first quadrant.
Theorem 5.2 is proved.

VI. BIFURCATION BEHAVIOR ANALYSIS

The system exhibits the following bifurcation characteristics:

- When $\alpha(w)K_2 < r_1$, the positive equilibrium E^* is stable, while E_2 is unstable.
- When $\alpha(w)K_2 > r_1$, E^* vanishes, and E_2 becomes stable.

At the critical condition $\alpha(w)K_2 = r_1$, the positive equilibrium E^* coincides with the boundary equilibrium $E_2(0, K_2)$, resulting in a transcritical bifurcation. The bifurcation condition corresponds to an eigenvalue crossing the imaginary axis:

$$\alpha(w_c)K_2 = r_1 \tag{16}$$

Substituting the saturated wind effect function $\alpha(w) = \alpha_0\left(1 + \frac{\delta w}{1+\kappa w}\right)$, we derive:

$$\alpha_0\left(1 + \frac{\delta w_c}{1 + \kappa w_c}\right)K_2 = r_1, \tag{17}$$

yielding the critical wind speed:

$$w_c = \frac{\frac{r_1}{\alpha_0 K_2} - 1}{\delta - \kappa\left(\frac{r_1}{\alpha_0 K_2} - 1\right)}. \tag{18}$$

Theorem 6.1. *When the parameters of system (1) satisfy the critical condition*

$$w = w_c \tag{19}$$

the system undergoes a transcritical bifurcation.
Proof. We verify the conditions of Sotomayor's theorem. At the equilibrium $E_2(0, K_2)$, the Jacobian matrix is:

$$J(E_2, w_c) = \begin{pmatrix} 0 & 0 \\ 0 & -r_2 \end{pmatrix}. \tag{20}$$

The matrix $J(E_2, w_c)$ has a zero eigenvalue. Let V and W be the eigenvectors corresponding to this eigenvalue for $J(E_2, w_c)$ and $J(E_2, w_c)^T$, respectively. Solving $J \cdot V = 0$:

$$\begin{pmatrix} 0 & 0 \\ 0 & -r_2 \end{pmatrix}\begin{pmatrix} v_1 \\ v_2 \end{pmatrix} = \begin{pmatrix} 0 \\ 0 \end{pmatrix} \implies V = \begin{pmatrix} 1 \\ 0 \end{pmatrix}, \tag{21}$$

and solving $W^T \cdot J = 0$:

$$\begin{pmatrix} w_1 & w_2 \end{pmatrix} \begin{pmatrix} 0 & 0 \\ 0 & -r_2 \end{pmatrix} = \begin{pmatrix} 0 & 0 \end{pmatrix} \implies W = \begin{pmatrix} 1 \\ 0 \end{pmatrix}. \tag{22}$$

Next, verify transversality conditions. The derivative of the system with respect to w is:

$$F_w = \begin{pmatrix} -N_1 N_2 \frac{d\alpha}{dw} \\ 0 \end{pmatrix} \implies F_w(E_2, w_c) = \begin{pmatrix} 0 \\ 0 \end{pmatrix}. \tag{23}$$

Left-multiplying by W^T:

$$W^T F_w(E_2, w_c) = \begin{pmatrix} 1 & 0 \end{pmatrix} \begin{pmatrix} 0 \\ 0 \end{pmatrix} = 0. \tag{24}$$

Compute the Jacobian DF_w:

$$DF_w(E_2, w_c) = \begin{pmatrix} -K_2 \frac{d\alpha}{dw} & 0 \\ 0 & 0 \end{pmatrix}, \tag{25}$$

thus

$$DF_w(E_2, w_c) \cdot V = \begin{pmatrix} -K_2 \cdot \frac{\alpha_0 \delta}{(1+\kappa w_c)^2} \\ 0 \end{pmatrix}, \tag{26}$$

and left-multiplying by W^T:

$$W^T [DF_w(E_2, w_c) \cdot V] = -K_2 \cdot \frac{\alpha_0 \delta}{(1+\kappa w_c)^2} \neq 0. \tag{27}$$

Finally, verify $W^T[D^2F(E_2, w_c)(V, V)] \neq 0$.

Compute the second derivative D^2F (Hessian matrix applied to vector V twice):

$$D^2F(V,V) = \begin{pmatrix} \frac{\partial^2 F_1}{\partial N_1^2} V_1^2 + 2 \frac{\partial^2 F_1}{\partial N_1 \partial N_2} V_1 V_2 + \frac{\partial^2 F_1}{\partial N_2^2} V_2^2 \\ \frac{\partial^2 F_2}{\partial N_1^2} V_1^2 + 2 \frac{\partial^2 F_2}{\partial N_1 \partial N_2} V_1 V_2 + \frac{\partial^2 F_2}{\partial N_2^2} V_2^2 \end{pmatrix}$$

For $F_1 = r_1 N_1 \left(1 - \frac{N_1}{K_1}\right) - \alpha(w) N_1 N_2$, the second derivatives are:

$$\frac{\partial^2 F_1}{\partial N_1^2} = -\frac{2r_1}{K_1}, \quad \frac{\partial^2 F_1}{\partial N_1 \partial N_2} = -\alpha(w), \quad \frac{\partial^2 F_1}{\partial N_2^2} = 0$$

For the second equation:

$$F_2 = r_2 N_2 \left(1 - \frac{N_2}{K_2}\right),$$

the second derivative of F_2 with respect to N_2 is:

$$\frac{\partial^2 F_2}{\partial N_2^2} = -\frac{2r_2}{K_2}, \quad \frac{\partial^2 F_2}{\partial N_1 \partial N_2} = 0, \quad \frac{\partial^2 F_2}{\partial N_1^2} = 0.$$

Substituting $V_1 = 1$ and $V_2 = 0$, we obtain:

$$\begin{aligned} & D^2F(E_2, w_c)(V,V) \\ = & \begin{pmatrix} -\frac{2r_1}{K_1} \cdot 1^2 + 2(-\alpha(w_c)) \cdot 1 \cdot 0 + 0 \cdot 0^2 \\ 0 \cdot 1^2 + 2 \cdot 0 \cdot 1 \cdot 0 + (-\frac{2r_2}{K_2}) \cdot 0^2 \end{pmatrix} \\ = & \begin{pmatrix} -\frac{2r_1}{K_1} \\ 0 \end{pmatrix} \end{aligned} \tag{28}$$

Multiplying by W^T:

$$\begin{aligned} & W^T[D^2F(E_2, w_c)(V,V)] \\ = & \begin{pmatrix} 1 & 0 \end{pmatrix} \begin{pmatrix} -\frac{2r_1}{K_1} \\ 0 \end{pmatrix} \\ = & -\tfrac{2r_1}{K_1} \neq 0. \end{aligned} \tag{29}$$

According to Sotomayor's theorem, when the system parameters satisfy the critical condition $w = w_c$, system (1) undergoes a transcritical bifurcation.

The proof of Theorem 6.1 is complete.

Finally, compute the second derivative D^2F applied to V twice:

$$D^2F(V,V) = \begin{pmatrix} -\frac{2r_1}{K_1} \\ 0 \end{pmatrix}.$$

Left-multiplying by W^T:

$$W^T[D^2F(E_2, w_c)(V,V)] = -\frac{2r_1}{K_1} \neq 0.$$

By Sotomayor's theorem, system (1) undergoes a transcritical bifurcation at $w = w_c$.
Theorem 6.1 is proved.

VII. NUMERICAL EXAMPLES

This section verifies the correctness of Theorems 5.1, 5.2, and 6.1 through numerical simulations.

Example 7.1 Set parameters: $r_1 = 1.0$, $r_2 = 0.5$, $K_1 = 100$, $K_2 = 50$, $\alpha_0 = 0.01$, $\delta = 0.5$, $\kappa = 0.1$.
(1) Take $w = 1.0$. Calculations yield: $\alpha(w) \approx 0.0145$, $\alpha(w)K_2 = 0.725 < r_1 = 1.0$. By Theorem 5.2, the positive equilibrium $E^*(27.5, 50)$ is globally attracting. Initial values: $(N_1(0), N_2(0)) = (10,5), (50,20), (80,40), (30,60)$, with $t \in [0, 50]$. Figure 1 and Figure 2 confirm the global stability of the positive equilibrium E^* under low wind speed.
(2) Set parameters: $w = 3.0$. Calculations yield: $\alpha(w) \approx 0.0215$, $\alpha(w)K_2 = 1.0725 > r_1 = 1.0$. By Theorem 5.1, the boundary equilibrium $E_2(0, 50)$ is globally attracting. Initial values remain unchanged. Figure 3 and Figure 4 confirm the extinction of the victim species under high wind speed.

(3) Critical case: Calculate $w_c = 2.5$. By Theorem 6.1, the positive equilibrium coincides with $E_2(0, K_2)$ at $w = w_c$. Initial values: $(N_1(0), N_2(0)) = (10,5), (80,20), (80,40), (80,70)$, with $t \in [0, 50]$. Figure 5 demonstrates the phase trajectory diagram for the critical case.

(4) Sensitivity analysis: Observe N_1^* versus w. Figure 6 shows that N_1^* monotonically decreases with increasing w. Despite saturation effects, excessive wind speed ultimately drives the victim population to extinction.

(5) Set the initial condition $(N_1(0), N_2(0)) = (10, 5)$, for $w = 0, 1, 2, 3$, we plot the phase trajectory of the solution(Fig. 7). From Figure 7, it can be observed that as w increases, the rate at which $N_1(t)$ decreases accelerates. When w becomes sufficiently large, $N_1(t)$ will eventually approach zero.

Example 7.2 The saturated wind effect involves three key parameters: α_0, δ, and κ. We now conduct a sensitivity analysis on these parameters. Set parameters: $r_1 = 1.0$, $r_2 = 0.5$, $K_1 = 100$, $K_2 = 50$, $w = 1.0$.

(1) Set $\alpha_0 = 0.01$, $\delta = 0.5$, and vary κ. We observe the relationship between N_1^* and κ. Figure 8 shows that

as κ increases, N_1^* monotonically increases. However, as κ continues to increase, the rate of increase in N_1^* gradually slows down. In Fig. 9, we take the initial value $(N_1(0), N_2(0)) = (30, 20)$ and plot the time series of $N_1(t)$ for different values of κ. As κ increases, $N_1(t)$ gradually rises, demonstrating that larger κ values favor the sustainable survival of the first population.

(2) Set $\kappa = 0.1$, $\delta = 0.5$, and vary α_0. We observe the relationship between N_1^* and α_0. Figure 13 shows that as α_0 increases, N_1^* monotonically decreases. A critical value exists; when α_0 exceeds this critical value, N_1^* becomes negative, which is biologically unrealistic. This indicates that in the system (1), α_0 is a critical parameter. To ensure the system's sustainability, α_0 must be constrained within a certain range. In Fig. 11, we take the initial value $(N_1(0), N_2(0)) = (30, 20)$ and plot the time series of $N_1(t)$ for different values of α_0. It can be observed that as α_0 gradually increases, $N_1(t)$ decreases correspondingly. When α_0 becomes sufficiently large, $N_1(t)$ tends to 0 as t increases, which indicates that larger α_0 values are unfavorable for the sustainable survival of the first population.

(3) Set $\kappa = 0.1$, $\alpha_0 = 0.01$, and vary δ. We observe the relationship between N_1^* and δ. Figure 12 shows that as δ increases, N_1^* monotonically decreases. A critical value exists; when δ exceeds this critical value, N_1^* becomes negative, which is biologically unrealistic. This indicates that in system (1), δ is a critical parameter in the saturated wind effect. If δ is too large, even though the impact on the population decreases as wind speed increases, it cannot prevent the eventual extinction of the population. In Fig. 13, we take the initial value $(N_1(0), N_2(0)) = (30, 20)$ and plot the time series of $N_1(t)$ for different values of δ. It can be observed that as δ gradually increases, $N_1(t)$ decreases correspondingly. When δ becomes sufficiently large, $N_1(t)$ tends to 0 as t increases, which indicates that larger δ values are unfavorable for the sustainable survival of the first population.

VIII. CONCLUSIONS AND DISCUSSION

A. Main conclusions

- **Equilibrium dynamics**: The system exhibits three boundary equilibria (E_0, E_1, E_2) and a conditional positive equilibrium E^*. Crucially, numerical simulations (Section VII) confirm that coexistence at E^* is achievable only when $\alpha(w)K_2 < r_1$, with victim population density N_1^* monotonically decreasing with wind speed w (Fig. 6). This aligns with Theorem 3.1 but adds empirical validation.
- **Bifurcation threshold**: The transcritical bifurcation at w_c (Eq. 30) is no longer theoretical; Example 7.1(3) visually demonstrates the collapse of E^* into E_2 when $w = w_c$ (Fig. 5), reinforcing Theorem 6.1 with phase-space analysis.
- **Saturation effects**: Simulations in Example 7.2 reveal that larger κ (saturation coefficient) mitigates wind-driven extinction (Fig. 8), while high δ or α_0 accelerates it (Figs. 10–13). This empirically quantifies the "nonlinear protection" hinted in Section II.

B. Ecological implications

- **Wind management**: The critical threshold w_c (Eq. 18) now has empirical support from Fig. 6. Practically, windbreaks should aim to maintain $w < w_c$, where $w_c = \frac{r_1/\alpha_0 K_2 - 1}{\delta - \kappa(r_1/\alpha_0 K_2 - 1)}$. Example 7.1(5) further shows rapid victim extinction when $w \geq 3.0$ (Fig. 3), suggesting a safety margin below w_c.
- **Parameter sensitivity**: The saturation coefficient κ emerges as a key lever for conservation. Fig. 9 shows that even modest κ increases (e.g., $\kappa = 0.1 \to 0.5$) can elevate N_1^* by $\sim 40\%$, while δ and α_0 require stricter control (Figs. 11, 13).

C. Expanded future work

- **Data integration**: Calibrate $\alpha(w)$ using field data (e.g., pathogen dispersal under wind gradients) to refine the saturation term $\frac{\delta w}{1+\kappa w}$. Example 7.2 motivates this by showing how κ and δ dominate outcomes.
- **Stochastic extensions**: Numerical results (e.g., Fig. 7's trajectory variability) suggest that stochastic wind fluctuations could trigger early extinction below w_c, warranting Ito-process modeling.
- **Spatial dynamics**: The monotonic $N_1^* - w$ relationship (Fig. 6) implies wind-driven spatial heterogeneity, urging reaction-diffusion extensions with advection terms.

This study establishes a theoretical framework for understanding wind-mediated amensalism. The results provide actionable insights for ecosystem conservation and highlight avenues for future interdisciplinary research.

REFERENCES

[1] X. Xi, J. N. Griffin, S. Sun, "Grasshoppers amensalistically suppress caterpillar performance and enhance plant biomass in an alpine meadow," *Oikos,* vol.122, no.7, pp. 1049-1057, 2013.

[2] Z. F. Zhu, Q. L. Chen, "Study on Lotka-Volterra amensalism model," *J. Jixi Univ. (Nat. Sci. Ed.)*, vol.8, no.5, pp. 100-101, 2008.

[3] X. Y. Guan, F. D. Chen, "Dynamical analysis of a two species amensalism model with Beddington–DeAngelis functional response and Allee effect on the second species," *Nonlinear Analysis: Real World Applications*, vol.48, no.1, pp. 71-93, 2019.

[4] J. M. Gómez, A. González-Megías, "Asymmetrical interactions between ungulates and phytophagous insects: being different matters," *Ecology*, vol.83, no.1, pp. 203-211, 2002.

[5] G. C. Sun, "Qualitative analysis on two populations amensalism model," *J. Jiamusi Univ. (Nat. Sci. Ed.)*, vol. 21, no.2, pp. 283-286, 2003.

[6] A. R. S. Abd Alhadi , R. K. Naji, "The contribution of amensalism and parasitism in the three-species ecological system's dynamic," *Commun. Math. Biol. Neurosci.*, vol. 2024, Article ID 33, 2024.

[7] X. Y. Huang, F. D. Chen, "The influence of the Allee effect on the dynamic behaviors of two species amensalism system with a refuge for the first species," *Adv. Appl. Math*, vol.8, no.6, pp. 1166-1180, 2019.

[8] M. Zhao, Y. Ma, Y. Du, "Global dynamics of an amensalism system with Michaelis-Menten type harvesting," *Electronic Research Archive*, vol.31, no.2, pp. 549-574, 2022.

[9] X. Guan, H. Deng, "The qualitative analysis of a two species ammenslism model with non-monotonic functional response and Allee effect on second specie," *Ann. of Appl. Math*, vol.35, no.2, pp. 126-138, 2019.

[10] Y. B. Chong, S. M. Chen, F. D. Chen, "On the existence of positive periodic solution of an amensalism model with Beddington-DeAngelis functional response," *WSEAS Trans. Math.*, vol.21, no.1, pp. 572-579, 2022.

[11] T. Y. Li, Q. R. Wang, “Stability and Hopf bifurcation analysis for a two species commensalism system with delay,” *Qual. Theory Dyn. Syst.*, vol. 20, article ID 83, 2021.

[12] B. G. Chen, “Dynamic behaviors of a non-selective harvesting Lotka-Volterra amensalism model incorporating partial closure for the populations,” *Adv. Differ. Equ.* , vol.2018, article ID 272, 2018.

[13] D. M. Luo, Q. R. Wang, “Global dynamics of a Holling-II amensalism system with nonlinear growth rate and Allee effect on the first species,” *Int. J. Bifurc. Chaos*, vol. 31, article ID 2150050, 2021.

[14] D. Luo, Y. Qiu, “Global Dynamics of a Holling-II Amensalism System with a Strong Allee Effect on the Harmful Species,” *International Journal of Bifurcation and Chaos*, vol.34, no.09, 2450115, 2024.

[15] H. Y. Liu, H. G. Yu, C. J. Dai, Z. Ma, Q. Wang, M. Zhao, “Dynamical analysis of an aquatic amensalism model with non-selective harvesting and Allee effect,” *Math. Biosci. Eng.*, vol.18, pp. 8857-8882, 2021.

[16] Z. Wei, Y. H. Xia, T. H. Zhang, “Stability and bifurcation analysis of an amensalism model with weak Allee effect,” *Qual. Theory Dyn. Syst.*, vol.19, 341, 2020.

[17] M. Zhao, Y. F. Du, “Stability and bifurcation analysis of an amensalism system with Allee effect,” *Adv. Differ. Equ.*, vol.2020, article ID 341, 2020.

[18] C. Q. Lei, “Dynamic behaviors of a stage structure amensalism system with a cover for the first species,” *Adv. Differ. Equ.*, vol.2018, article ID 272, 2018.

[19] Y. Liu, L. Zhao, X. Y. Huang, H. Deng, “Stability and bifurcation analysis of two species amensalism model with Michaelis-Menten type harvesting and a cover for the first species,” *Adv. Differ. Equ.*, vol 2018, article ID 295, 2018.

[20] X. D. Xie, F. D. Chen, M. X. He, “Dynamic behaviors of two species amensalism model with a cover for the first species,” *J. Math. Comput. Sci.*, vol.16, no.2, pp. 395-401, 2016.

[21] D. Luo, Q. Wang, “Global dynamics of a Beddington–DeAngelis amensalism system with weak Allee effect on the first species,” *Applied Mathematics and Computation*, vol. 408, article ID 126368, 2021.

[22] F. Chen, Y. Chen, Z. Li, et al. “Note on the persistence and stability property of a commensalism model with Michaelis–Menten harvesting and Holling type II commensalistic benefit,” *Applied Mathematics Letters*, vol.134, article ID 108381, 2022.

[23] Z. Zhang, “Stability and bifurcation analysis for a amensalism system with delays,” *Mathematica Numerica Sinica*, vol.30, no.1, pp. 213–224, 2008.

[24] R. X. Wu, L. Zhao, Q. X. Lin, “Stability analysis of a two species amensalism model with Holling II functional response and a cover for the first species,” *J. Nonlinear Funct. Anal.*, vol.2016, no.46, pp. 1-15, 2016.

[25] R. Wu, “Dynamic behaviors of a nonlinear amensalism model,” *Advances in Difference Equations*, vol. 2018, Article number: 187, pp. 1-13, 2018.

[26] R. Wu, “A two species amensalism model with non-monotonic functional response,” *Commun. Math. Biol. Neurosci.*, vol. 2016, Article ID 19, 2016.

[27] X. Guo, L. Ding, Y. Hui, et al., “Dynamics of an amensalism system with strong Allee effect and nonlinear growth rate in deterministic and fluctuating environment,” *Nonlinear Dynamics*, vol.112, no.23, pp. 21389-21408, 2024.

[28] Q. Zhou, F. Chen, “Dynamical analysis of a discrete amensalism system with the Beddington–DeAngelis functional response and Allee effect for the unaffected species,” *Qualitative Theory of Dynamical Systems*, vol.22, no.1, 16, 2023.

[29] Q. Zhou, F. Chen, S. Lin, “Complex dynamics analysis of a discrete amensalism system with a cover for the first species,” *Axioms*, vol.11, no.8, article ID 365, 2022.

[30] Q .Q. Su, F. D. Chen, “The influence of partial closure for the populations to a non-selective harvesting Lotka-Volterra discrete amensalism model,” *Adv. Differ. Equ.*, vol.29, article ID 281, 2019.

[31] R. Y. Han, Y. L. Xue, L. Y. Yang, et al, “On the existence of positive periodic solution of a Lotka-Volterra amensalism model,” *Journal of Rongyang University*, vol.33, no.2, pp. 22–26, 2015.

[32] Q. Zhu, F. Chen, Z. Li, et al. “Global dynamics of two-species amensalism model with Beddington–DeAngelis functional response and fear effect,” *International Journal of Bifurcation and Chaos*, vol.34, no.06, 2450075, 2024.

[33] A. Ditta, P. A. Naik, R. Ahmed, et al. “Exploring periodic behavior and dynamical analysis in a harvested discrete-time commensalism system,” *International Journal of Dynamics and Control*, vol.13, no.2, pp. 1-12, 2025.

[34] Q. Li, F. Chen, L. Chen, et al. “Dynamical analysis of a discrete amensalism system with Michaelis–Menten type harvesting for the second species,” *Qualitative Theory of Dynamical Systems*, vol. 23(Suppl 1), article ID 279, 2024.

[35] Q. Zhou, F. Chen, “Dynamical analysis of a discrete amensalism system with the Beddington–DeAngelis functional response and Allee effect for the unaffected species,” *Qualitative Theory of Dynamical Systems*, vol.22, no.1, article ID 16, 2023.

[36] Q. Zhou, Y. Chen, S. Chen, et al. “Dynamic analysis of a discrete amensalism model with Allee effect,” *J. Appl. Anal. Comput*, vol.13, no. 5, pp. 2416-2432, 2023.

[37] X. Hu, H. Li, F. Chen, “Bifurcation analysis of a discrete amensalism model,” *International Journal of Bifurcation and Chaos*, vol.34, no.02, 2450020, 2024.

[38] X. R. Li, Q. Yue, F. D. Chen, “The dynamic behaviors of nonselective harvesting Lotka-Volterra predator-prey system with partial closure for populations and the fear effect of the prey species,” *IAENG International Journal of Applied Mathematics*, vol. 53, no. 3, pp.818-825, 2023.

[39] C. P. Huang, F. D. Chen, Q. Zhu, Q. Q. Li, “How the wind changes the Leslie-Gower predator-prey system?,” *IAENG International Journal of Applied Mathematics,* vol. 53, no.3, pp. 907-915, 2023.

[40] Z. Zhu, F. Chen, L. Lai, et al. “Dynamic behaviors of a discrete May type cooperative system incorporating Michaelis-Menten type harvesting,” *IAENG International Journal of Applied Mathematics*, vol. 50, no.3, pp. 458-467, 2020.

[41] Z. Zhu, R. Wu, F. Chen, et al. “Dynamic behaviors of a Lotka-Volterra commensal symbiosis model with non-selective Michaelis-Menten type harvesting,” *IAENG International Journal of Applied Mathematics*, vol. 50, no.2, pp.396-404, 2020.

[42] K. Fang, J. Chen, Z. Zhu, et al. “Qualitative and bifurcation analysis of a single species Logistic model with Allee effect and feedback control,” *IAENG International Journal of Applied Mathematics*, vol. 52, no. 2, pp. 320-326, 2022.

[43] M. He, Z. Li, F. Chen, et al. “Dynamic behaviors of an N-species Lotka-Volterra model with nonlinear impulses,” *IAENG International Journal of Applied Mathematics*, vol.50, no.1, pp. 22-30, 2020.

[44] Y. Chong, Y. Hou, S. Chen S, et al. “The influence of fear effect to the dynamic behaviors of Lotka-Volterra ammensalism model,” *Engineering Letters*, vol.32, no.6, pp. 1233-1242, 2024.

[45] Y. Chong, Q. Zhu, Q. Li, et al. “Dynamic behaviors of a two species amensalism model with a second species dependent cover,” *Engineering Letters*, vol. 32, no. 8, pp. 1553-1561, 2024.

[46] E. Klimczuk, L. Halupka, B. Czyz, et al. “Factors driving variation in biparental incubation behaviour in the reed warbler Acrocephalus scirpaceus, ” *Ardea*, vol.103, no.1, pp.51-59, 2015.

[47] S. Jawad, D. Sultan, M. Winter, “The dynamics of a modified Holling-Tanner prey-predator model with wind effect, ” *International Journal of Nonlinear Analysis and Applications*, vol. 12(Special Issue): pp. 2203-2210, 2021.

[48] C. Huang, F. Chen, Q. Zhu, et al. “How the wind changes the Leslie-Gower predator-prey system?,” *IAENG International Journal of Applied Mathematics*, vol. 53, no.3, pp. 907-915, 2023.

[49] M. J. Cherry, B. T. Barton, “Effects of wind on predator-prey interactions, ” *Food Webs,* vol.13, no.1, pp. 92-97, 2017.

[50] D. Barman, V. Kumar, J. Roy, et al. “Modeling wind effect and herd behavior in a predator-prey system with spatiotemporal dynamics, ” *The European Physical Journal Plus*, vol.137, no.8, 950-960, 2022.

[51] D. Barman, J. Roy, S. Alam, “Impact of wind in the dynamics of prey-predator interactions,” *Mathematics and Computers in Simulation*, vol.191, no.1, pp. 49-81, 2022.

[52] P. Panja, “Impacts of wind and anti-predator behaviour on predator-prey dynamics: a modelling study,” *International Journal of Computing Science and Mathematics*, vol.15, no.4, pp. 396-407, 2022.

[53] Y. C. Zhou, Z. Jin, J. L. Qin, “Ordinary Differential Equation and Its Application”[M], Beijing, Science Press, 2003.

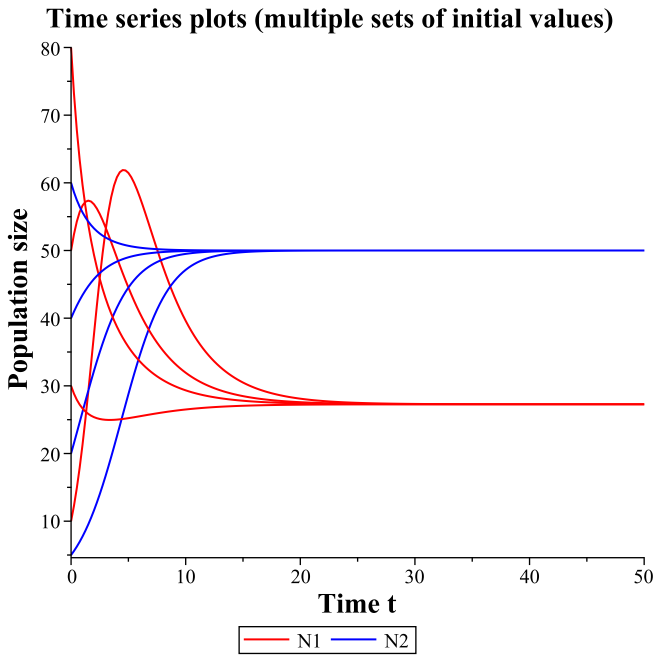

Fig. 1: Time series plots for Example 7.1, case (1).

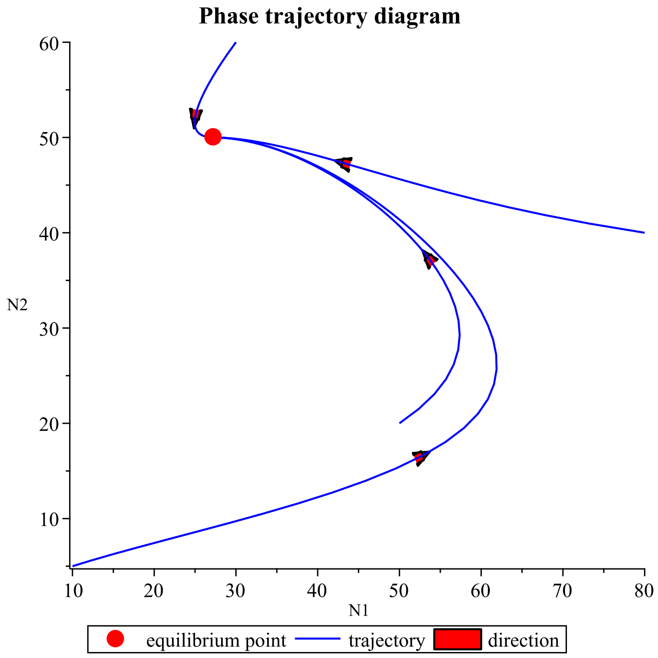

Fig. 2: Phase trajectory diagram for Example 7.1, case (1).

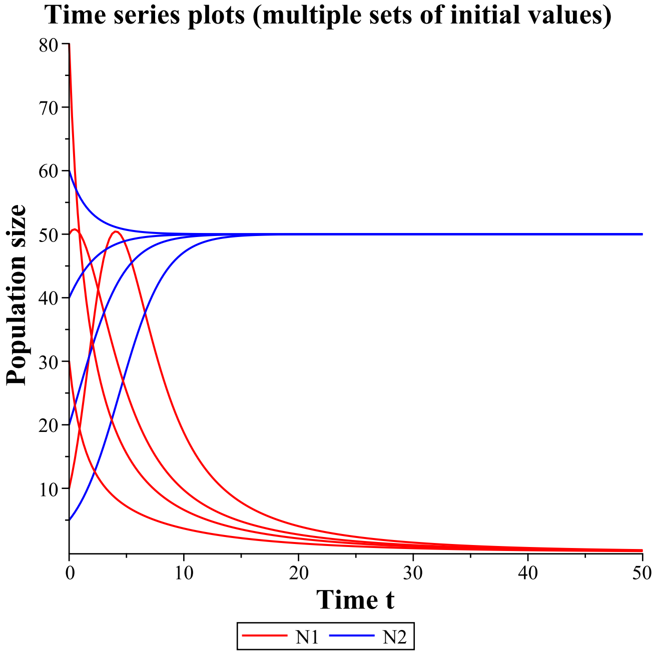

Fig. 3: Time series plots for Example 7.1, case (2).

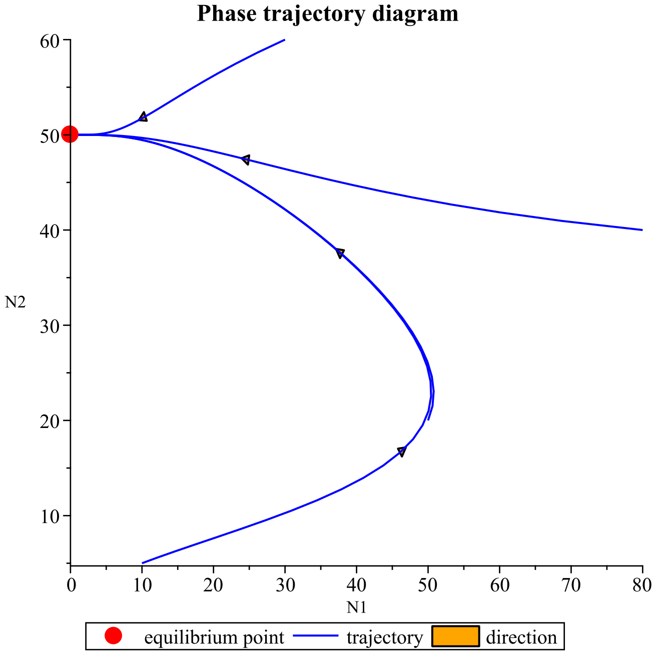

Fig. 4: Phase trajectory diagram for Example 7.1, case (2).

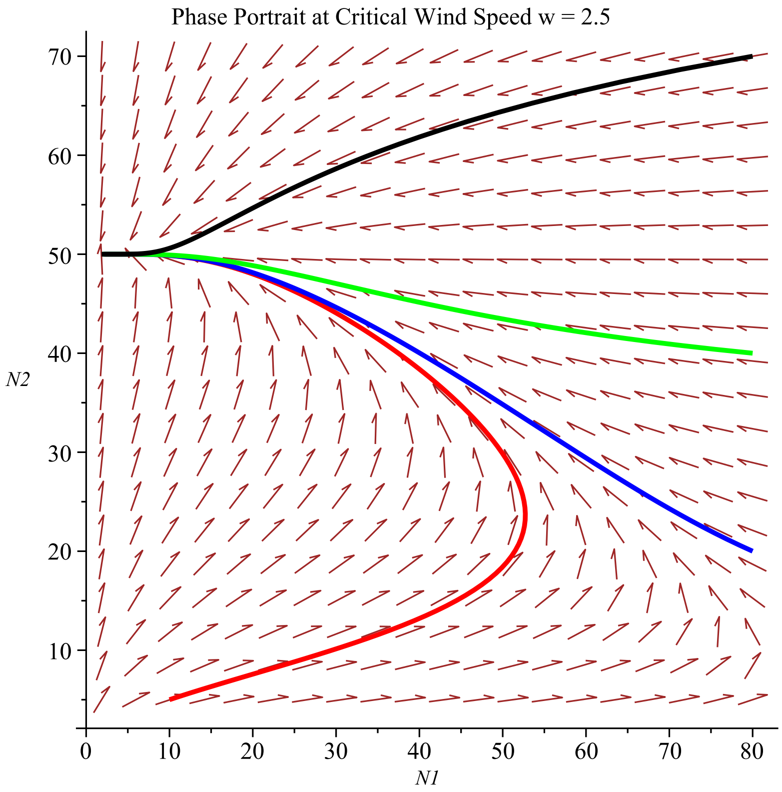

Fig. 5: Phase trajectory diagram for Example 7.1, case (3).

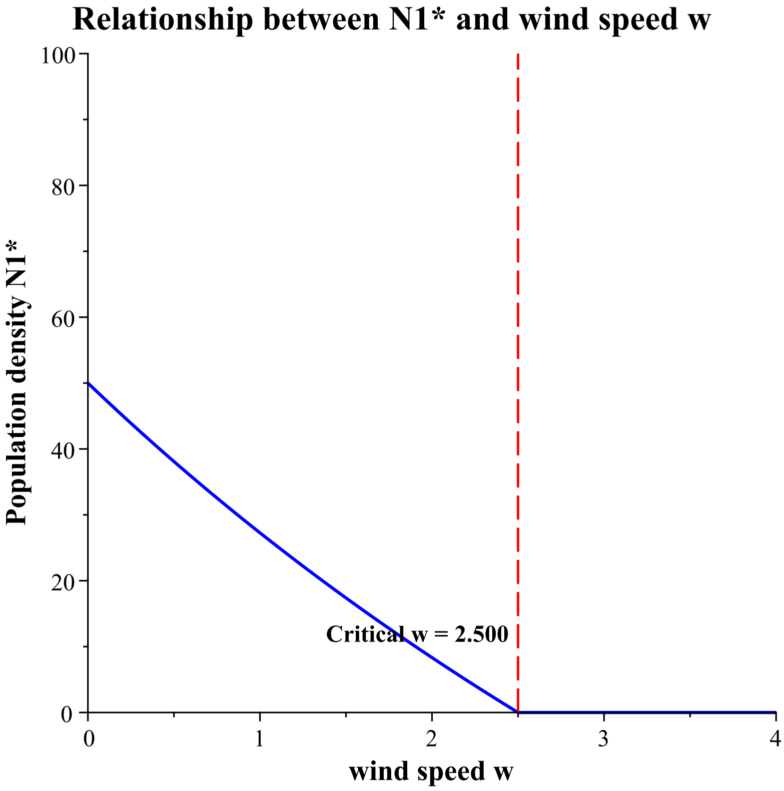

Fig. 6: Relationship between N_1^* and wind speed w for Example 7.1, case (4).

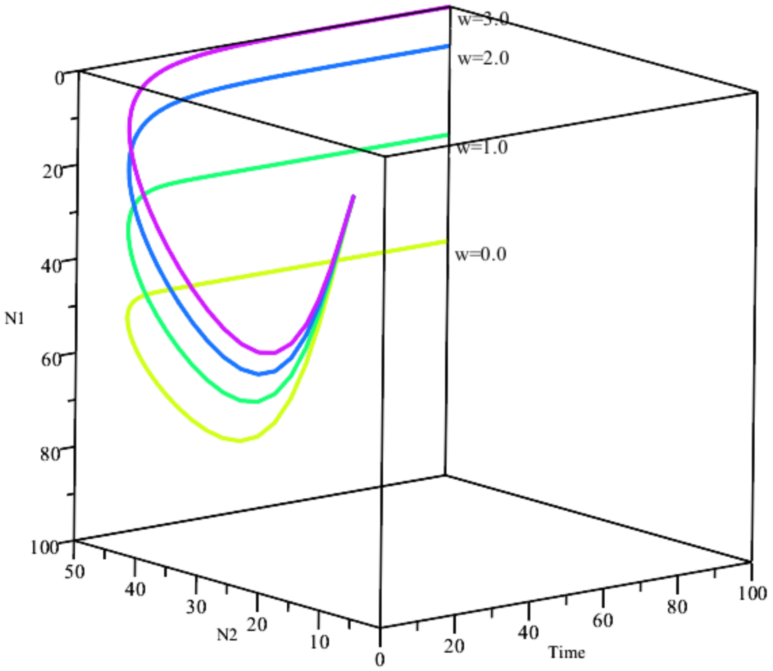

Fig. 7: Phase trajectories for different wind speed for Example 7.1, case (5).

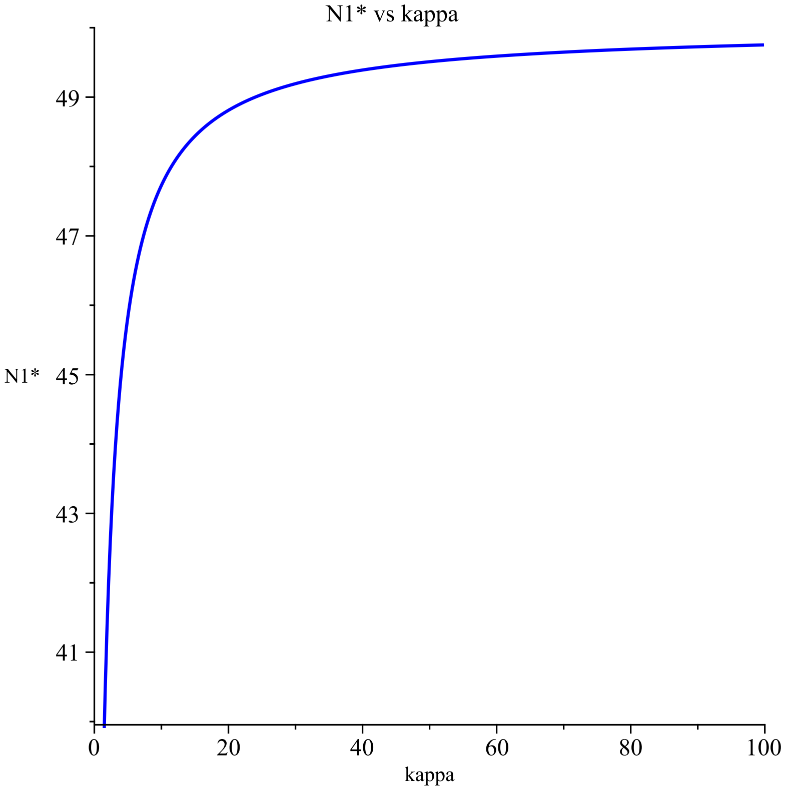

Fig. 8: Relationship between N_1^* and κ in Example 7.2, case (1).

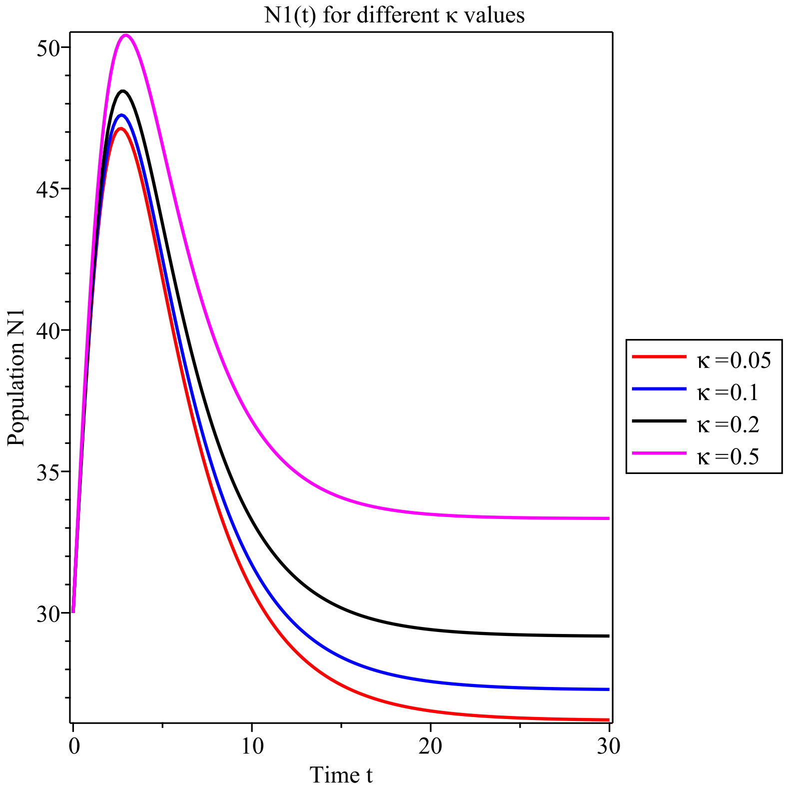

Fig. 9: N1(t) for different κ values in Example 7.2, case (1).

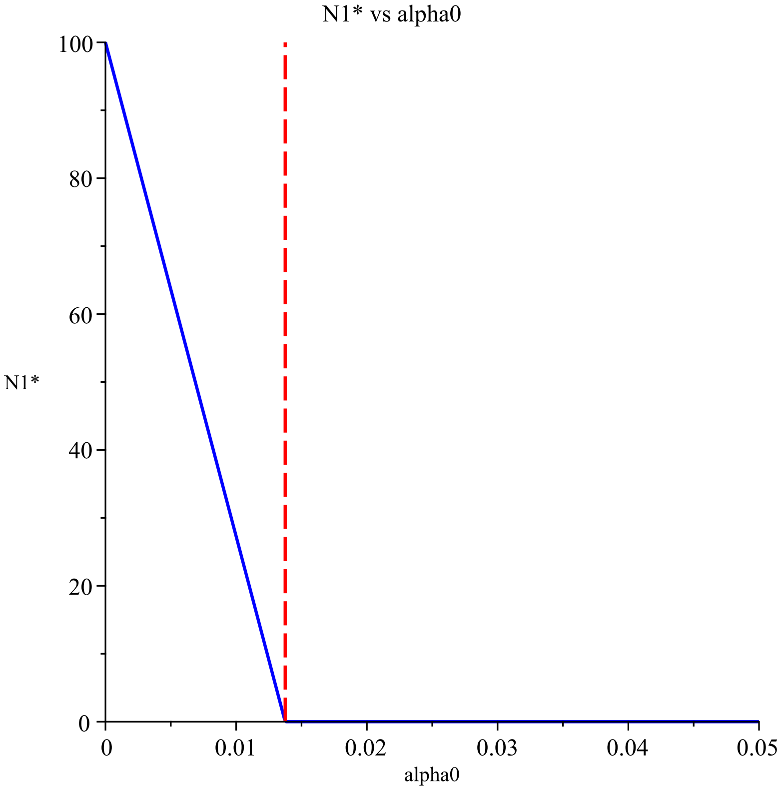

Fig. 10: Relationship between N_1^* and α_0 in Example 7.2, case (2).

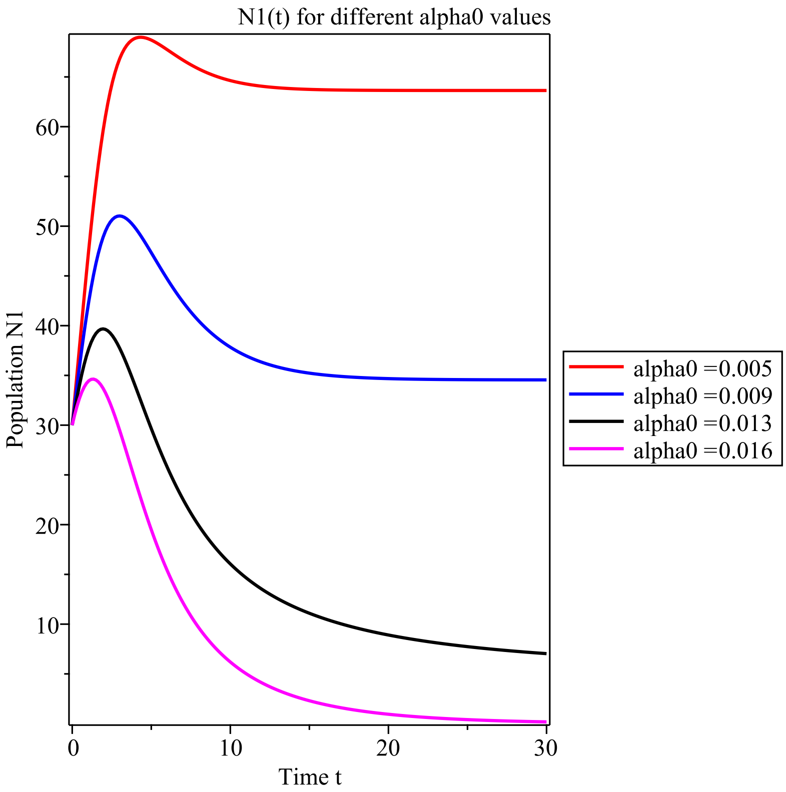

Fig. 11: N1(t) for different kappa values in Example 7.2, case (2).

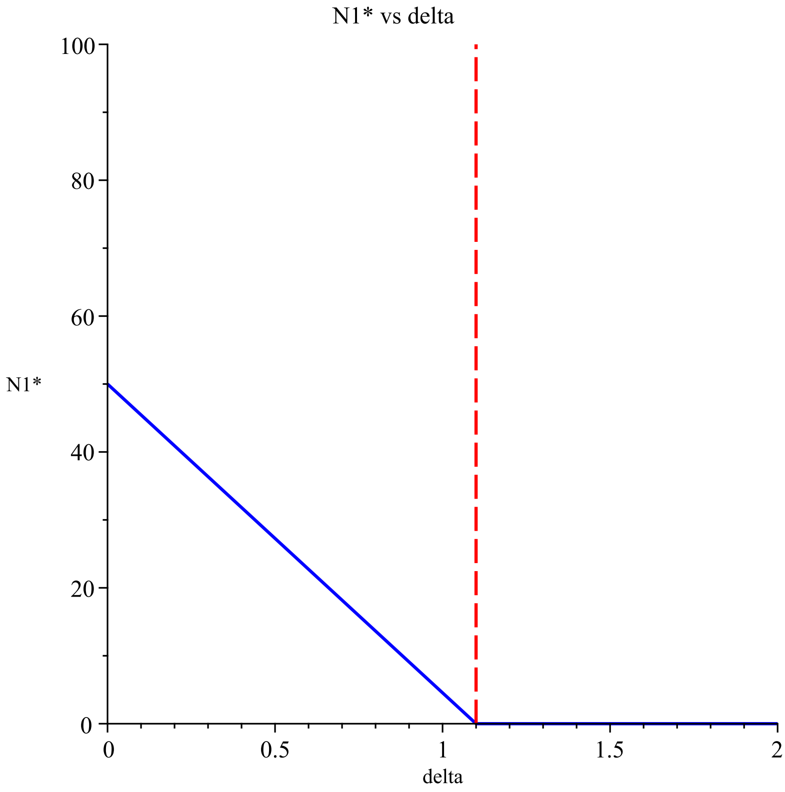

Fig. 12: Relationship between N_1^* and δ in Example 7.2.

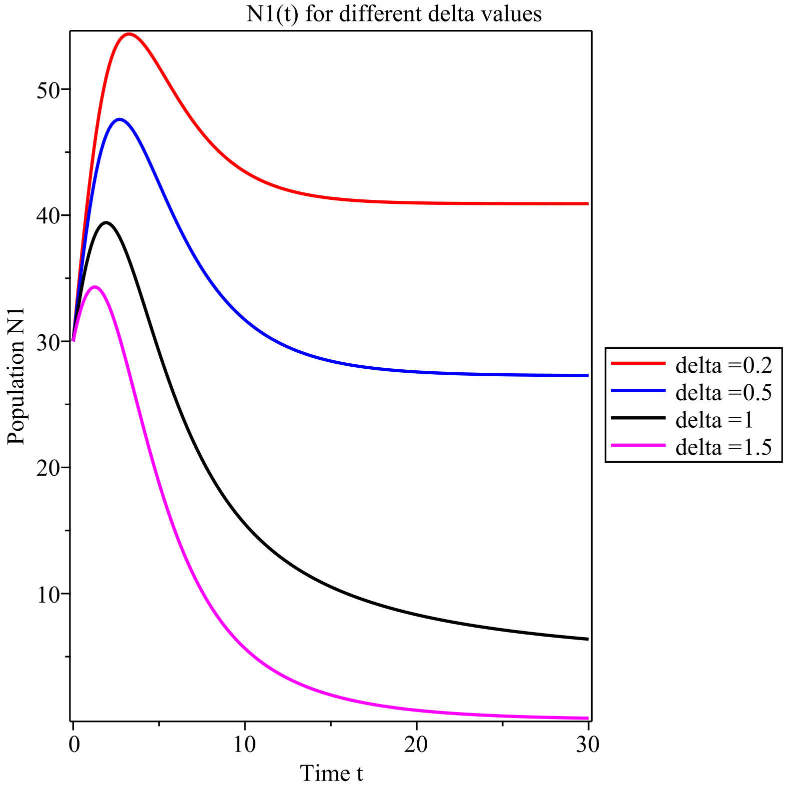

Fig. 13: N1(t) for different δ values in Example 7.2, case (3).